C. R. Physique 15 (2014) 403–414

Contents lists available at ScienceDirect

Comptes Rendus Physique

www.sciencedirect.com

Electromagnetism / Électromagnétisme

Quasi-local transmission conditions for non-overlapping domain decomposition methods for the Helmholtz equation

Conditions de transmission quasi-locales pour des méthodes de décomposition de domaine appliquées à l'équation de Helmholtz

Matthieu Lecouvez [a,*], Bruno Stupfel [a], Patrick Joly [b], Francis Collino [b]

[a] *Commissariat à l'énergie atomique (CEA), 15, avenue des Sablières, 33114 Le Barp, France*
[b] *POEMS, UMR CNRS/ENSTA/INRIA, ENSTA ParisTech, 828, bd des Maréchaux, 91762 Palaiseau cedex, France*

ARTICLE INFO

Article history:
Available online 3 May 2014

Keywords:
Scattering
Domain decomposition
Transmission conditions
Riesz potential

Mots-clés :
Diffusion
Domaine de décomposition
Transmission (conditions)
Potentiel de Riesz

ABSTRACT

In this article, we present new transmission conditions for a domain decomposition method, applied to a scattering problem. Unlike other conditions used in the literature, the conditions developed here are non-local, but can be written as an integral operator (as a Riesz potential) on the interface between two domains. This operator, of order $\frac{1}{2}$, leads to an exponential convergence of the domain decomposition algorithm. A spectral analysis of the influence of the operator on simple cases is presented, as well as some numerical results and comparisons.

RÉSUMÉ

Nous présentons dans cet article de nouvelles conditions de transmission pour une méthode de décomposition de domaine appliquée au problème de la diffraction. À l'inverse d'autres conditions décrites dans la littérature, celles développées ici ne sont pas locales, mais peuvent s'écrire sous la forme d'un opérateur intégral (tel qu'un potentiel de Riesz) à l'interface entre deux domaines. Cet opérateur, d'ordre $\frac{1}{2}$, conduit à une convergence exponentielle de l'algorithme de décomposition de domaine. Une analyse spectrale de l'influence de l'opérateur portant sur des cas simples est presentée, ainsi que quelques résultats numériques et comparaisons.

1. Introduction

Scattering problems by electrically large objects occur in many domains. Numerical computation of this kind of problem remains limited by resources (computational time, memory) because of the large number of unknowns, especially when inhomogeneous materials are present. Domain decomposition methods are of great interest in a finite elements context. The

* Corresponding author.
E-mail address: matthieu.lecouvez@cea.fr (M. Lecouvez).

http://dx.doi.org/10.1016/j.crhy.2014.04.005
1631-0705/

problem is decomposed into several coupled subproblems, which can be solved independently. This reduces the memory required and makes parallel computation easier.

New interfaces are created to split the domain into several subdomains, thus new conditions are required on these interfaces to get a well-posed problem in each subdomain. Moreover, the conditions on the new interfaces (or transmission conditions) directly determine the rate of convergence of the domain decomposition algorithm.

Several studies have been made regarding these domain decomposition methods, particularly on the transmission conditions. One can mention the transmission conditions of Després [1], which are a specific linear combination of Dirichlet and Neumann conditions, or conditions using higher order of derivatives as in [2] or [3]. Some conditions also involve operators like rational fractions as in [4]. However, all these conditions do not have the properties allowing a theoretical proof of the geometric convergence of iterative domain decomposition algorithms.

2. General theory of domain decomposition

In this section, we extend the general theory developed in [5] to the case where the transmission operator has a real and an imaginary parts. We strictly keep their conventions and notations.

Let Ω be a closed domain and Γ its interface. $L^2(\Omega)$, respectively $L^2(\Gamma)$, denotes the space of square integrable functions defined on Ω, resp. Γ. The Hilbert spaces $H^m(\Omega)$, where m is an integer, is defined as the space of square integrable functions whose derivatives are also square integrable up to the order m. Hilbert spaces of fractional order are classically defined through the Fourier transform:

$$H^s(\Omega) = \left\{u \in L^2(\Omega) \text{ such that } \mathcal{F}^{-1}\left[\left(1+\xi^2\right)^{\frac{s}{2}}\mathcal{F}(u)\right] \in L^2(\Omega)\right\} \tag{1}$$

The problem consists in finding $u \in H^1(\Omega)$ such that:

$$(\mathcal{P}) \qquad \begin{cases} -\Delta u - \omega^2 u = f & \text{in } \Omega \\ \partial_n u + \mathrm{i}\omega u = h & \text{on } \Gamma \end{cases} \tag{2}$$

If $f \in L^2(\Omega)$ and $h \in L^2(\Gamma)$, then there exists a unique solution to the problem, such that $\Delta u \in L^2(\Omega)$ and $\partial_n u \in L^2(\Gamma)$. We now introduce a non-overlapping partition of Ω: $(\Omega_k)_{k=1..K}$. We note $\Sigma_{kj} = \Omega_k \cap \Omega_j$ the interface between the two domains. The restriction of quantities to the domain Ω_k (respectively Σ_{kj}) will be denoted with subscripts k (respectively kj). With these notations, the initial problem $(\mathcal{P})$ is equivalent to the collection of problems:

$$(\mathcal{P}_k) \qquad \begin{cases} -\Delta u_k - \omega^2 u_k = f_k & \text{in } \Omega_k \\ \partial_{n_k} u_k + \mathrm{i}\omega u_k = h_k & \text{on } \Sigma_{kk} \\ u_k = u_j & \text{on } \Sigma_{kj} \\ \partial_{n_k} u_k = -\partial_{n_j} u_j & \text{on } \Sigma_{kj} \end{cases} \tag{3}$$

Let $T_{r,kj}$ and $T_{i,kj}$ two real operators defined on Σ_{kj}. We assume that $T_{r,kj}$ can be written as $\Lambda_{kj}^* \Lambda_{kj}$ (where * denotes the adjoint operator), and that it is injective, where Λ_{kj} is an isometry from $H^s(\Sigma_{kj})$ into $L^2(\Sigma_{kj})$, for some $s > 0$:

$$T_{r,kj} : H^s(\Sigma_{kj}) \xrightarrow{\Lambda} L^2(\Sigma_{kj}) \xrightarrow{\Lambda} H^{-s}(\Sigma_{kj}) \tag{4}$$

We set $T_{r,kk} = I$ and $T_{i,kk} = 0$. We also assume that $T_{r,jk} = T_{r,kj}$ and $T_{i,jk} = -T_{i,kj}$, so that $T_{kj} = T_{r,kj} + \mathrm{i}T_{i,kj} = \overline{T_{jk}}$.

We define the following problems:

$$(\mathcal{P}'_k) \qquad \begin{cases} -\Delta u_k - \omega^2 u_k = f_k & \text{in } \Omega_k \\ \partial_{n_k} u_k + \mathrm{i}\omega u_k = h_k & \text{on } \Sigma_{kk} \\ \partial_{n_k} u_k + \mathrm{i}\omega T_{kj} u_k = -\partial_{n_j} u_j + \mathrm{i}\omega T_{kj} u_j & \text{on } \Sigma_{kj} \end{cases} \tag{5}$$

The equivalence between $(\mathcal{P}_k)$ and $(\mathcal{P}'_k)$, and thus the well-posedness of $(\mathcal{P}'_k)$ are ensured by the injectivity of $T_{r,kj}$. Indeed, as soon as $T_{r,kj}$ is injective, then the transmission conditions of $(\mathcal{P}'_k)$ imply that $u_k = u_j$ and $\partial_{n_k} u_k = -\partial_{n_j} u_j$ on Σ_{kj} and then the problem $(\mathcal{P}'_k)$ as a unique solution. Let us remark that this general framework contains most of the transmission conditions proposed in the literature. For instance:

- if $T_{kj} = I$, one recovers the original method proposed by Després [1];
- if T_{kj} is a second-order boundary differential operator (for instance Hodge's operator, which just becomes in the Helmholtz equation a double tangential derivative: ∂_τ^2), one gets the conditions of [3].

We now assume that the interfaces Σ_{kj} are closed manifolds and that Λ_{kj} is an isomorphism from $H^{1/2}(\Sigma_{kj})$ into $L^2(\Sigma_{kj})$, i.e. $s = \frac{1}{2}$. Under these assumptions, and using the results proven in [5], the convergence of the iterative algorithm using these transmission conditions is geometric.

For simplicity, we will now use operators $T_{kj} = z\Lambda^*\Lambda$ where z is a complex constant, and Λ verifies all previous conditions for geometric convergence.

3. Operators form $H^{1/2}(\Sigma)$ into $L^2(\Sigma)$

The condition $s = \frac{1}{2}$ for Λ prevents us from defining the operator with partial derivatives. The operator is a pseudo-differential operator that can be defined thanks to integral kernels. We look for an operator from $H^{1/2}(\mathbb{R}^d)$ where d is the dimension of Σ ($d = 2$ for 3D problems, $d = 1$ for 2D problems). To build such an operator, we use the Fourier transform $u(x) \in L^2(\mathbb{R}^d) \to \widehat{u}(k) \in L^2(\mathbb{R}^d)$. The symbol of the operator must verify:

$$C_-\left(1+|k|^2\right)^{\frac{1}{4}} \leq \left|\widehat{\Lambda}(k)\right| \leq C_+\left(1+|k|^2\right)^{\frac{1}{4}} \tag{6}$$

where C_- and C_+ are the constants. Let us study the operator Λ_0 whose symbol is $|k|^{\frac{1}{2}}$ (one can note that it does not verify the condition (6) since $\widehat{\Lambda_0}(0) = 0$). We decompose it as follows:

$$\widehat{\Lambda_0}(k) = |k|^{\frac{1}{2}} = -\mathrm{i}k \cdot \left(|k|^{-\frac{3}{2}}\mathrm{i}k\right) \tag{7}$$

This decomposition allows us to write, if the inverse Fourier transform of $|k|^{-\frac{3}{2}}$ is an integral kernel $\mathcal{K}_0$:

$$\Lambda_0 u(x) = -\mathrm{div}\int_{\mathbb{R}^d} \mathcal{K}_0\left(|x-y|\right)\nabla u(y)\mathrm{d}y \tag{8}$$

or in a bilinear form:

$$(\Lambda_0 u, v) = \int_{\mathbb{R}^d}\int_{\mathbb{R}^d} \mathcal{K}_0\left(|x-y|\right)\nabla u(y)\nabla v(x)\mathrm{d}x\mathrm{d}y \tag{9}$$

This kernel $\mathcal{K}_0$ belongs to the class of the Riesz potentials [6], which correspond to a fractional power of the operator $-\Delta$. In particular:

$$\mathcal{K}_0 = \frac{C(d, \frac{3}{2})}{|x|^{d-\frac{3}{2}}} \tag{10}$$

with $C(1, \frac{3}{2}) = -\sqrt{\frac{\pi}{2}}$ and $C(2, \frac{3}{2}) = 2\Gamma(\frac{3}{4})$ constants. Finally, we will use operators $\Lambda = \alpha I + \beta\Lambda_0$.

3.1. Case where Σ is of dimension 1

In this case, the operator is written as:

$$(\Lambda_0 u, v) = -\sqrt{\frac{\pi}{2}}\int_\Sigma\int_\Sigma |x-y|^{\frac{1}{2}}\nabla u(y)\nabla v(x)\mathrm{d}x\mathrm{d}y \tag{11}$$

3.2. Case where Σ is of dimension 2

In this case, the operator is written as:

$$(\Lambda_0 u, v) = 2\Gamma\left(\frac{3}{4}\right)\int_\Sigma\int_\Sigma \frac{\nabla u(y)\nabla v(x)\mathrm{d}x\mathrm{d}y}{|x-y|^{\frac{1}{2}}} \tag{12}$$

3.3. Truncation of the operator

The main inconvenient of that type of operators (or more generally of any operator verifying the conditions required to get a geometric convergence) is its non-locality. After discretization, they lead to full matrices, and thus to an important cost to invert them. To overcome this problem, one can introduce a truncation function χ_δ in the integrand provided that the function is smooth enough. This truncation will keep the integrand untouched around the diagonal $x = y$ and will nullify it far from the diagonal. It is a function of the distance $r = |x-y|$. To keep the appropriate behavior of the Fourier transform at infinity, the truncation function has to be at least c^2. One can take, for instance:

$$\begin{cases} \chi_\delta(r) = \chi\left(\dfrac{r}{\delta}\right) \\ \chi(r) = 1, \quad \forall r \in [0,1] \\ \chi(r) = 0, \quad \forall r \geq 2 \\ \chi(r) = \left(6r^2 - 9r + 4\right)(2-r)^3, \quad \forall r \in [1,2] \end{cases} \tag{13}$$

δ being a parameter governing the locality of the operator. Small values of δ will give very local operators (and thus very sparse matrices).

4. Discretization of a local problem

The local problem writes as following. Find $u_k \in H^1(\Omega_k)$ such that:

$$\begin{cases} -\Delta u_k - \omega^2 u_k = f_k & \text{in } \Omega_k \\ \partial_n u_k + \mathrm{i}\omega z \Lambda^2 u_k = g_k^{\text{in}} & \text{on } \partial\Omega_k = \Sigma_k \end{cases} \tag{14}$$

with the operator Λ:

$$(\Lambda u, v) = \alpha(u, v) + \beta \int_\Sigma \int_\Sigma \mathcal{K}_0\big(|x-y|\big)\chi_\delta\big(|x-y|\big)\nabla u(y)\nabla v(x)\mathrm{d}x\mathrm{d}y \tag{15}$$

This local problem depends on an incoming data g_k^{in}. This data comes from the neighbor domains Ω_j of the domain Ω_k. This is why we introduce the outgoing data $g_k^{\text{out}} = -\partial_n u_k + \mathrm{i}\omega\bar{z}\Lambda^2 u_k = -g_k^{\text{in}} + 2\mathrm{i}\omega\mathcal{R}(z)\Lambda^2 u_k$. At the iteration l of an iterative process, this quantity g_k^{out} is computed and will be used as the incoming data g_j^{in} at the next iteration $l+1$.

To solve the local problem, we introduce intermediate variables $\varphi = \Lambda u \in L^2(\Sigma)$. Let (Ψ_n) be the basis function associated with u and (Φ_m) those associated with φ in a finite-element context. We write:

$$u = \sum_n u_n \Psi_n, \qquad \varphi = \sum_m \varphi_m \Phi_m \tag{16}$$

The weak formulation of the problem can be written:

$$\begin{cases} \displaystyle\int_\Omega \big(\nabla u \nabla \widetilde{u} - \omega^2 u\widetilde{u}\big)\mathrm{d}x + \mathrm{i}\omega z(\Lambda\varphi, \widetilde{u})_\Sigma = \int_\Omega f\widetilde{u} + (g_{\text{in}}, \widetilde{u})_\Sigma & \forall \widetilde{u} \in H^1(\Omega) \\ (\varphi, \widetilde{\varphi})_\Sigma = (\Lambda u, \widetilde{\varphi})_\Sigma & \forall \widetilde{\varphi} \in L^2(\Sigma) \end{cases} \tag{17}$$

Let us define the following matrices:

$$\mathbb{M}_{i,j} = \int_\Omega \Psi_i \cdot \Psi_j, \qquad \mathbb{K}_{i,j} = \int_\Omega \nabla\Psi_i \cdot \nabla\Psi_j, \qquad \mathbb{M}_{\Sigma_{i,j}} = \int_\Sigma \Phi_i \cdot \Phi_j \tag{18}$$

$$\mathbb{B}_{i,j} = \alpha(\Phi_i, \Psi_j)_\Sigma + \beta \int_\Sigma \int_\Sigma |x-y|^{\frac{1}{2}} \chi_\delta\big(|x-y|\big)\nabla\Phi_i(y)\nabla\Psi_j(x)\mathrm{d}x\mathrm{d}y \tag{19}$$

and the following vector:

$$b_i = \int_\Omega f \cdot \Psi_i + (g_{\text{in}}, \Psi_i)_\Sigma \tag{20}$$

With these notations, the local system can be written in a matrix form:

$$\mathbb{A}_k \cdot \begin{bmatrix} \mathbf{u} \\ \varphi \end{bmatrix} = \begin{bmatrix} \mathbb{K} - w^2\mathbb{M} & \mathrm{i}\omega z\mathbb{B} \\ \mathbb{B}^T & \mathbb{M}_\Sigma \end{bmatrix} \cdot \begin{bmatrix} \mathbf{u} \\ \varphi \end{bmatrix} = \begin{bmatrix} \mathbf{b} \\ 0 \end{bmatrix} \tag{21}$$

u is defined on the whole domain, and thus the matrices $\mathbb{K}$ and $\mathbb{M}$ are $N_{\text{v}} * N_{\text{v}}$ where N_{v} is the total number of vertices. φ is defined on the interfaces only, thus $\mathbb{M}_\Sigma$ is $N_{\text{b}} * N_{\text{b}}$ where N_{b} is the number of vertices on the boundaries. These three matrices are sparse. $\mathbb{B}$ is $N_{\text{v}} * N_{\text{b}}$ and is full if no truncation is made. When adding truncation, one will sparsify this matrix.

The global iterative process to solve the global problem would write:

1. Start with $g_k^{\text{in}} = 0$ for all k,
2. Form the right-hand side $\mathbf{b}$ and solve every local system $\mathbb{A}_k$,
3. Form the quantity $g_k^{\text{out}} = -g_k^{\text{in}} + 2\mathrm{i}\omega\mathcal{R}(z)\Lambda^2 u_k$,
4. In each domain, exchange the quantity g_k^{out} with the neighbors and put the received data in g_k^{in},
5. Iterate to point 2. while the stopping criterion is not verified (e.g., residual norm of the error).

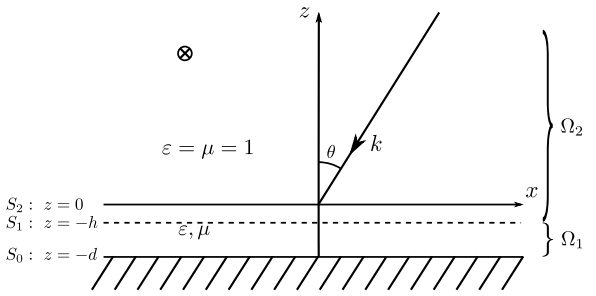

Fig. 1. Geometry of the problem.

5. Spectral analysis on an infinite plane

We consider a 1D problem (translationally invariant along the axes x and y, z being the third axis in this section) as presented in Fig. 1. It is made of a free infinite half-space ($z > 0$) and a material layer of thickness d ($-d < z < 0$). An impedance boundary condition is prescribed in $z = -d$. Moreover, the domain can possibly be closed by an absorbing boundary condition in $z = H$. The domain is excited by a plane wave $u = \mathrm{e}^{\mathrm{i}(k_x x + k_{0z} z + 2\pi f t/c)}$ with $k_x^2 + k_{0z}^2 = k_0^2$. $k_0 = \frac{2\pi f}{c}$ is the free-space wave number and $k = k_0\sqrt{\mu\varepsilon}$ is the wave number in the material, c being the speed of light in the free space. In the material, we also have $k^2 = k_x^2 + k_z^2$. We denote $s = k_x/k_0$ the mode of the wave.

Maxwell's equations write, in each polarization:

$$\text{TE:}\begin{cases} \left(\dfrac{\partial^2}{\partial x^2} + \dfrac{\partial^2}{\partial z^2} + k^2\right) E_y = 0, \qquad E_x = E_z = 0 \\ H_x = \dfrac{1}{\mathrm{i}k_0\mu}\dfrac{\partial}{\partial z} E_y \\ H_z = -\dfrac{1}{\mathrm{i}k_0\mu}\dfrac{\partial}{\partial x} E_y \\ H_y = 0 \end{cases} \tag{22}$$

$$\text{TM:}\begin{cases} \left(\dfrac{\partial^2}{\partial x^2} + \dfrac{\partial^2}{\partial z^2} + k^2\right) H_y = 0, \qquad H_x = H_z = 0 \\ E_x = -\dfrac{1}{\mathrm{i}k_0\varepsilon}\dfrac{\partial}{\partial z} H_y \\ E_z = \dfrac{1}{\mathrm{i}k_0\varepsilon}\dfrac{\partial}{\partial x} H_y \\ E_y = 0 \end{cases} \tag{23}$$

5.1. Solution to the exact problem

In this section, no decomposition domain is applied: the problem is solved globally. In each part (free space and material), the solution can be written as the sum of an incoming and outgoing wave:

$$\left(A(s)\mathrm{e}^{\mathrm{i}k_z(s)z} + B(s)\mathrm{e}^{-\mathrm{i}k_z(s)z}\right)\mathrm{e}^{\mathrm{i}k_0 s x} \tag{24}$$

In particular, in the free space, and with no absorbing condition, $A(s) = A_s^{\mathrm{v}} = 1$ and $B(s) = B_s^{\mathrm{v}} = R_s$ is the reflection coefficient. In the material, the coefficients $A(s) = A_s^{\mathrm{m}}$ and $B(s) = B_s^{\mathrm{m}}$ depend only on s and on the geometry of the problem. The continuity of the tangential fields in $z = 0$, the absorbing boundary condition and the impedance condition gives us the four equations needed to solve the problem. One can formulate it in matrix form:

$$\underbrace{\begin{bmatrix} \varphi_s & 1 & 0 & 0 \\ 1 & 1 & -1 & -1 \\ 1 & -1 & -\gamma_s & \gamma_s \\ 0 & 0 & \varphi_{\mathrm{ABC}} & 1 \end{bmatrix}}_{P_s} \cdot \begin{bmatrix} B_s^{\mathrm{m}} \\ A_s^{\mathrm{m}} \\ B_s^{\mathrm{v}} \\ A_s^{\mathrm{v}} \end{bmatrix} = \begin{bmatrix} 0 \\ 0 \\ 0 \\ 1 \end{bmatrix} \tag{25}$$

with, for each polarization with absorbing boundary conditions (ABC):

$$\text{TE:}\begin{cases}\varphi_s = \dfrac{1+Z\frac{k_z}{k_0\mu}}{1-Z\frac{k_z}{k_0\mu}}\mathrm{e}^{2\mathrm{i}k_z d} = \dfrac{\mu+Z\sqrt{\mu\varepsilon-s^2}}{\mu-Z\sqrt{\mu\varepsilon-s^2}}\mathrm{e}^{2\mathrm{i}k_0 d\sqrt{\mu\varepsilon-s^2}}\\ \gamma_s = \dfrac{k_{0z}\mu}{k_z} = \mu\dfrac{\sqrt{1-s^2}}{\sqrt{\mu\varepsilon-s^2}}\\ \varphi_{\mathrm{ABC}} = \dfrac{1-Z_{\mathrm{ABC}}\frac{k_{0z}}{k_0}}{1+Z_{\mathrm{ABC}}\frac{k_{0z}}{k_0}}\mathrm{e}^{-2\mathrm{i}k_{0z}H} = \dfrac{1-Z_{\mathrm{ABC}}\sqrt{1-s^2}}{1+Z_{\mathrm{ABC}}\sqrt{1-s^2}}\mathrm{e}^{-2\mathrm{i}k_0 H\sqrt{1-s^2}}\end{cases} \tag{26}$$

$$\text{TM:}\begin{cases}\varphi_s = \dfrac{Z+\frac{k_z}{k_0\varepsilon}}{Z-\frac{k_z}{k_0\varepsilon}}\mathrm{e}^{2\mathrm{i}k_z d} = \dfrac{Z\varepsilon+\sqrt{\mu\varepsilon-s^2}}{Z\varepsilon-\sqrt{\mu\varepsilon-s^2}}\mathrm{e}^{2\mathrm{i}k_0 d\sqrt{\mu\varepsilon-s^2}}\\ \gamma_s = \dfrac{k_{0z}\varepsilon}{k_z} = \varepsilon\dfrac{\sqrt{1-s^2}}{\sqrt{\mu\varepsilon-s^2}}\\ \varphi_{\mathrm{ABC}} = \dfrac{Z_{\mathrm{ABC}}-\frac{k_{0z}}{k_0}}{Z_{\mathrm{ABC}}+\frac{k_{0z}}{k_0}}\mathrm{e}^{-2\mathrm{i}k_{0z}H} = \dfrac{Z_{\mathrm{ABC}}-\sqrt{1-s^2}}{Z_{\mathrm{ABC}}+\sqrt{1-s^2}}\mathrm{e}^{-2\mathrm{i}k_0 H\sqrt{1-s^2}}\end{cases} \tag{27}$$

With no ABC (infinite half free space), it suffices to take $\varphi_{\mathrm{ABC}} = 0$. One can note that TM polarization consists in TE polarization with the change of parameters:

$$(\mu, \varepsilon, Z, Z_{\mathrm{ABC}}) \to \left(\varepsilon, \mu, \frac{1}{Z}, \frac{1}{Z_{\mathrm{ABC}}}\right) \tag{28}$$

From Eq. (25), one can calculate the determinant of the system, as well as the exact solution of the problem.

$$\det P_s = -\big[\varphi_s(\gamma_s+1)-(\gamma_s-1)\big] - \varphi_{\mathrm{ABC}}\big[\varphi_s(\gamma_s-1)-(\gamma_s+1)\big] \tag{29}$$

$$\begin{bmatrix} B_s^{\mathrm{m}} \\ A_s^{\mathrm{m}} \\ B_s^{\mathrm{v}} \\ A_s^{\mathrm{v}} \end{bmatrix} = \frac{1}{\det P_s}\begin{bmatrix} 2\gamma_s \\ -2\gamma_s\varphi_s \\ \varphi_s(1-\gamma_s)+1+\gamma_s \\ -[\varphi_s(\gamma_s+1)-(\gamma_s-1)] \end{bmatrix} \tag{30}$$

5.2. Transmission conditions

From now on, we will consider only TM polarization. We split the domain into two subdomains by a new interface located in $z=-h$, with $-d<-h<0<H$. The interface is in the material. We consider a transmission operator $\mathcal{B}u = \frac{1}{\varepsilon}\partial_n u + \mathrm{i}k_0 T u$. The two transmission conditions are:

$$\begin{cases}\dfrac{1}{\varepsilon}\partial_z u_1 + \mathrm{i}k_0(T_r+\mathrm{i}T_i)u_1 = \dfrac{1}{\varepsilon}\partial_z u_2 + k_0(T_r+\mathrm{i}T_i)u_2\\ -\dfrac{1}{\varepsilon}\partial_z u_2 + \mathrm{i}k_0(T_r-\mathrm{i}T_i)u_2 = -\dfrac{1}{\varepsilon}\partial_z u_1 + k_0(T_r-\mathrm{i}T_i)u_1\end{cases} \tag{31}$$

The function $\mathrm{e}^{\mathrm{i}k_0 sx}$ is an eigenvector of the operator T, i.e. $T(\mathrm{e}^{\mathrm{i}k_0 sx}) = \widehat{t_s}\mathrm{e}^{\mathrm{i}k_0 sx}$. So the two previous equations can be decomposed on the basis $\mathrm{e}^{\mathrm{i}k_0 sx}$. One gets after some simplifications:

$$\begin{aligned} &A_{s,1}^{\mathrm{m}}\left[\frac{\mathrm{i}k_z}{\varepsilon}+\mathrm{i}k_0\widehat{t_s}\right] + B_{s,1}^{\mathrm{m}}\left[-\frac{\mathrm{i}k_z}{\varepsilon}+\mathrm{i}k_0\widehat{t_s}\right]\mathrm{e}^{2\mathrm{i}k_z h} = A_{s,2}^{\mathrm{m}}\left[\frac{\mathrm{i}k_z}{\varepsilon}+\mathrm{i}k_0\widehat{t_s}\right] + B_{s,2}^{\mathrm{m}}\left[-\frac{\mathrm{i}k_z}{\varepsilon}+\mathrm{i}k_0\widehat{t_s}\right]\mathrm{e}^{2\mathrm{i}k_z h}\\ &A_{s,1}^{\mathrm{m}}\left[-\frac{\mathrm{i}k_z}{\varepsilon}+\mathrm{i}k_0\widehat{\overline{t}_s}\right] + B_{s,1}^{\mathrm{m}}\left[\frac{\mathrm{i}k_z}{\varepsilon}+\mathrm{i}k_0\widehat{\overline{t}_s}\right]\mathrm{e}^{2\mathrm{i}k_z h} = A_{s,2}^{\mathrm{m}}\left[-\frac{\mathrm{i}k_z}{\varepsilon}+\mathrm{i}k_0\widehat{\overline{t}_s}\right] + B_{s,2}^{\mathrm{m}}\left[\frac{\mathrm{i}k_z}{\varepsilon}+\mathrm{i}k_0\widehat{\overline{t}_s}\right]\mathrm{e}^{2\mathrm{i}k_z h}\end{aligned} \tag{32}$$

Thanks to these two last equations, one can form the global system with transmission conditions:

$$\underbrace{\begin{bmatrix} \varphi_s & 1 & 0 & 0 & 0 & 0 \\ \psi_{1,s} & 1 & -\psi_{1,s} & -1 & 0 & 0 \\ \psi_{2,s} & 1 & -\psi_{2,s} & -1 & 0 & 0 \\ 0 & 0 & 1 & 1 & -1 & -1 \\ 0 & 0 & 1 & -1 & -\gamma_s & \gamma_s \\ 0 & 0 & 0 & 0 & \varphi_{\mathrm{ABC}} & 1 \end{bmatrix}}_{K_s} \cdot \underbrace{\begin{bmatrix} B_{s,2}^{\mathrm{m}} \\ A_{s,2}^{\mathrm{m}} \\ B_{s,1}^{\mathrm{m}} \\ A_{s,1}^{\mathrm{m}} \\ B_s^{\mathrm{v}} \\ A_s^{\mathrm{v}} \end{bmatrix}}_{x_s} = \underbrace{\begin{bmatrix} 0 \\ 0 \\ 0 \\ 0 \\ 0 \\ 1 \end{bmatrix}}_{f_s} \tag{33}$$

where

$$\psi_{1,s} = \frac{-\frac{k_z}{\varepsilon} + k_0\widehat{t_s}}{\frac{k_z}{\varepsilon} + k_0\widehat{t_s}} e^{2ik_z h}, \qquad \psi_{2,s} = \frac{\frac{k_z}{\varepsilon} + k_0\overline{\widehat{t_s}}}{-\frac{k_z}{\varepsilon} + k_0\overline{\widehat{t_s}}} e^{2ik_z h}. \tag{34}$$

Once again, we can compute the determinant of the new system:

$$\det K_s = (\psi_{2,s} - \psi_{1,s}) \det P_s \tag{35}$$

We can see that the new system is invertible, assuming that the original system is invertible, if and only if $\psi_{s,1} \neq \psi_{s,2} \Leftrightarrow \mathcal{R}(\widehat{t_s}) \neq 0$.

5.3. Decomposition domain algorithms

An iterative process is introduced through two different algorithms: the Jacobi and Gauss–Seidel ones, both in their relaxed form. For the Jacobi algorithm, the transmission conditions are:

$$\text{Jacobi: } \begin{cases} \mathcal{B}_1 u_1^{l+1} = (1 - r_1)\mathcal{B}_1 u_1^l + r_1 \mathcal{B}_1 u_2^l \\ \mathcal{B}_2 u_2^{l+1} = r_2 \mathcal{B}_2 u_1^l + (1 - r_2)\mathcal{B}_2 u_2^l \end{cases} \tag{36}$$

where r_1 and r_2 are relaxation coefficients, and for the Gauss–Seidel one:

$$\text{Gauss–Seidel: } \begin{cases} \mathcal{B}_1 u_1^{l+1} = (1 - r_1)\mathcal{B}_1 u_1^l + r_1 \mathcal{B}_1 u_2^l \\ \mathcal{B}_2 u_2^{l+1} = r_2 \mathcal{B}_2 u_1^{l+1} + (1 - r_2)\mathcal{B}_2 u_2^l \end{cases} \tag{37}$$

In both cases, we can split the matrix K_s into $K_s = M_s - N_s$, and the iterative algorithm becomes:

$$M_s x_s^{l+1} = N_s x_s^l + f_s \tag{38}$$

The iterative matrix $M_s^{-1} N_s$ governs the algorithm, and the convergence rate of the algorithm is directly linked to its eigenvalues. Indeed, the convergence rate of the algorithms is $\rho_s = \max |\lambda_s|$, where λ_s are the eigenvalues of $M_s^{-1} N_s$. For more generalities on the Jacobi or Gauss–Seidel iterative methods, the reader is referred to [7].

5.3.1. Jacobi algorithm

For the Jacobi algorithm, K_s is split into $K_s = M_s - N_s$, where M_s corresponds to the block diagonal part of K_s. Each diagonal block of M_s is the spectral equivalent of each local problem $\mathbb{A}_k$ of the previous sections. The diagonal structure of M_s means that in transmission conditions, we use data computed for the previous iteration only:

$$K_s = M_s - N_s, \qquad x_s^{l+1} = M_s^{-1} N_s x_s^l + M_s^{-1} f_s \tag{39}$$

with:

$$M_s = \begin{bmatrix} \varphi_s & 1 & 0 & 0 & 0 & 0 \\ \frac{\psi_{1,s}}{r_1} & \frac{1}{r_1} & 0 & 0 & 0 & 0 \\ 0 & 0 & -\frac{\psi_{2,s}}{r_2} & -\frac{1}{r_2} & 0 & 0 \\ 0 & 0 & 1 & 1 & -1 & -1 \\ 0 & 0 & 1 & -1 & -\gamma_s & \gamma_s \\ 0 & 0 & 0 & 0 & \varphi_{\text{ABC}} & 1 \end{bmatrix} \tag{40}$$

$$N_s = \begin{bmatrix} 0 & 0 & 0 & 0 & 0 & 0 \\ \psi_{1,s}(\frac{1}{r_1} - 1) & \frac{1}{r_1} - 1 & -\psi_{1,s} & -1 & 0 & 0 \\ -\psi_{2,s} & -1 & -\psi_{2,s}(\frac{1}{r_2} - 1) & -(\frac{1}{r_2} - 1) & 0 & 0 \\ 0 & 0 & 0 & 0 & 0 & 0 \\ 0 & 0 & 0 & 0 & 0 & 0 \\ 0 & 0 & 0 & 0 & 0 & 0 \end{bmatrix} \tag{41}$$

The only non-zero eigenvalues are:

$$\lambda_s^{\text{J}}(r_1, r_2, Q_s) = 1 - \frac{r_1 + r_2}{2} \pm \frac{1}{2}\sqrt{(r_1 - r_2)^2 + 4 r_1 r_2 Q_s} \tag{42}$$

where:

$$Q_s = \frac{(\psi_{2,s} - \varphi_s)(\psi_{1,s} - \Gamma_s)}{(\psi_{1,s} - \varphi_s)(\psi_{2,s} - \Gamma_s)}, \qquad \Gamma_s = \frac{\varphi_{\text{ABC}}(\gamma_s + 1) + \gamma_s - 1}{\varphi_{\text{ABC}}(\gamma_s - 1) + \gamma_s + 1} \tag{43}$$

5.3.2. Gauss–Seidel algorithm

For the Gauss–Seidel algorithm, K_s is split into $K_s = M_s - N_s$, where M_s corresponds to the lower block triangular part of K_s. Each diagonal block of M_s is still the spectral equivalent of each local problem $\mathbb{A}_k$ of the previous sections. The lower part of M_s just means that at a specific iteration l, we use data computed at the previous iteration $l-1$ as well as some already computed data of the current iteration l:

$$K_s = M_s - N_s, \qquad x_s^{l+1} = M_s^{-1} N_s x_s^l + M_s^{-1} f_s \tag{44}$$

with:

$$M_s = \begin{bmatrix} \varphi_s & 1 & 0 & 0 & 0 & 0 \\ \frac{\psi_{1,s}}{r_1} & \frac{1}{r_1} & 0 & 0 & 0 & 0 \\ \psi_{2,s} & 1 & -\frac{\psi_{2,s}}{r_2} & -\frac{1}{r_2} & 0 & 0 \\ 0 & 0 & 1 & 1 & -1 & -1 \\ 0 & 0 & 1 & -1 & -\gamma_s & \gamma_s \\ 0 & 0 & 0 & 0 & \varphi_{\mathrm{ABC}} & 1 \end{bmatrix} \tag{45}$$

$$N_s = \begin{bmatrix} 0 & 0 & 0 & 0 & 0 & 0 \\ \psi_{1,s}(\frac{1}{r_1} - 1) & \frac{1}{r_1} - 1 & -\psi_{1,s} & -1 & 0 & 0 \\ 0 & 0 & -\psi_{2,s}(\frac{1}{r_2} - 1) & -(\frac{1}{r_2} - 1) & 0 & 0 \\ 0 & 0 & 0 & 0 & 0 & 0 \\ 0 & 0 & 0 & 0 & 0 & 0 \\ 0 & 0 & 0 & 0 & 0 & 0 \end{bmatrix} \tag{46}$$

The only non-zero eigenvalues are:

$$\lambda_s^{\mathrm{GS}}(r_1, r_2, Q_s) = 1 - \frac{r_1 + r_2}{2} + \frac{r_1 r_2}{2} Q_s \pm \frac{1}{2}\sqrt{(r_1 - r_2)^2 - 2r_1 r_2 (r_1 + r_2 - 2) Q_s + r_1^2 r_2^2 Q_s^2} \tag{47}$$

where we also have:

$$Q_s = \frac{(\psi_{2,s} - \varphi_s)(\psi_{1,s} - \Gamma_s)}{(\psi_{1,s} - \varphi_s)(\psi_{2,s} - \Gamma_s)}, \qquad \Gamma_s = \frac{\varphi_{\mathrm{ABC}}(\gamma_s + 1) + \gamma_s - 1}{\varphi_{\mathrm{ABC}}(\gamma_s - 1) + \gamma_s + 1} \tag{48}$$

5.3.3. Some analysis

First of all, we can see that if $r_1 = r_2 = 1$ (i.e. no relaxation is applied) then $\rho_s^{\mathrm{J}} = |\sqrt{Q_s}|$ and $\rho_s^{\mathrm{GS}} = |Q_s|$. A Gauss–Seidel algorithm would require twice fewer iteration than a Jacobi algorithm. More generally, a Gauss–Seidel algorithm is expected to be more efficient than a Jacobi algorithm.

Besides, we observe that $Q_s = 1 \Rightarrow \rho_s = 1$ for both methods, and any relaxation coefficient. Moreover, $Q_s = 1$ is equivalent to $\varphi_s = \Gamma_s$ (i.e. $\det P_s = 0$ and the initial system is ill posed), or $\psi_{1,s} = \psi_{2,s}$ (i.e. $\mathcal{R}(\widehat{t_s}) = 0$ and the problems $\mathcal{P}_k$ of Eq. (3) and $\mathcal{P}'_k$ of Eq. (5) are not equivalent). The analytic computation of $\lim Q_s$ for large modes ($s \to \infty$) shows that if $\mathcal{R}(\widehat{t_s}) \not\sim |s|$ for large s, we get:

$$\lim_{s\to\infty} Q_s = 1 \tag{49}$$

and thus $\lim \rho_s = 1$ for all methods and parameters. This behavior was expected and shows that only appropriate operators can lead to geometric convergence.

6. Spectral analysis on a circle

The same developments made on the plane surface can be made on a circle. We still consider a 2D problem (translationally invariant along y) made of a circular conductor of radius R_0 covered with a homogeneous material layer of thickness d. We write $R_2 = R_0 + d$. Again, an absorbing boundary condition (ABC) is prescribed in $R_3 = R_2 + H$. The thickness of each component of the domain is thus taken identical as the infinite plane case. Maxwell's equations are written in cylindrical coordinates and reduce to Helmholtz equation. The general solution is decomposed on the basis $\mathrm{e}^{\mathrm{i}m\theta}$, where m is the mode of the wave, and can be written (equivalently to Eq. (24)):

$$\big(A_m J_m(kr) + B_m Y_m(kr)\big)\mathrm{e}^{\mathrm{i}m\theta} \tag{50}$$

where J_m and Y_m are the Bessel functions of the first and second kind. We write A_m^{m} and B_m^{m} the coefficients in the material, and A_m^{v} and B_m^{v} the coefficients in vacuum. As previously, the continuity of the tangential fields in $r = R_2$, the ABC in $r = R_3$, and the impedance boundary condition (IBC) in $r = R_0$ give the four equations required to solve the problem. The system is really similar to the previous case, see Eq. (25):

$$\underbrace{\begin{bmatrix} \varphi_m & 1 & 0 & 0 \\ 1 & \alpha_m & -\beta_m & -\gamma_m \\ 1 & \alpha'_m & -\beta'_m & -\gamma'_m \\ 0 & 0 & \varphi_{\mathrm{ABC}} & 1 \end{bmatrix}}_{P_m} \cdot \begin{bmatrix} B_m^{\mathrm{m}} \\ A_m^{\mathrm{m}} \\ B_m^{\mathrm{v}} \\ A_m^{\mathrm{v}} \end{bmatrix} = \begin{bmatrix} 0 \\ 0 \\ 0 \\ \mathrm{i}^{\mathrm{m}} \end{bmatrix} \tag{51}$$

with, for each polarization:

$$\text{TE:} \begin{cases} \varphi_m = \dfrac{Y_m(kR_0) + \mathrm{i}Z\sqrt{\frac{\varepsilon}{\mu}}Y'_m(kR_0)}{J_m(kR_0) + \mathrm{i}Z\sqrt{\frac{\varepsilon}{\mu}}J'_m(kR_0)} \\ \alpha_m = \dfrac{J_m(kR_2)}{Y_m(kR_2)} \\ \beta_m = \dfrac{Y_m(k_0R_2)}{Y_m(kR_2)} \\ \gamma_m = \dfrac{J_m(k_0R_2)}{Y_m(kR_2)} \\ \alpha'_m = \dfrac{J'_m(kR_2)}{Y'_m(kR_2)} \\ \beta'_m = \dfrac{Y'_m(k_0R_2)}{\sqrt{\frac{\varepsilon}{\mu}}Y'_m(kR_2)} \\ \gamma'_m = \dfrac{J'_m(k_0R_2)}{\sqrt{\frac{\varepsilon}{\mu}}Y'_m(kR_2)} \\ \varphi_{\mathrm{ABC}} = \dfrac{Y_m(k_0R_3) - \mathrm{i}Z_{\mathrm{ABC}}Y'_m(k_0R_3)}{J_m(k_0R_3) - \mathrm{i}Z_{\mathrm{ABC}}J'_m(k_0R_3)} \end{cases} \qquad \text{TM:} \begin{cases} \varphi_m = \dfrac{ZY_m(kR_0) + \mathrm{i}\sqrt{\frac{\mu}{\varepsilon}}Y'_m(kR_0)}{ZJ_m(kR_0) + \mathrm{i}\sqrt{\frac{\mu}{\varepsilon}}J'_m(kR_0)} \\ \alpha_m = \dfrac{J_m(kR_2)}{Y_m(kR_2)} \\ \beta_m = \dfrac{Y_m(k_0R_2)}{Y_m(kR_2)} \\ \gamma_m = \dfrac{J_m(k_0R_2)}{Y_m(kR_2)} \\ \alpha'_m = \dfrac{J'_m(kR_2)}{Y'_m(kR_2)} \\ \beta'_m = \dfrac{Y'_m(k_0R_2)}{\sqrt{\frac{\mu}{\varepsilon}}Y'_m(kR_2)} \\ \gamma'_m = \dfrac{J'_m(k_0R_2)}{\sqrt{\frac{\mu}{\varepsilon}}Y'_m(kR_2)} \\ \varphi_{\mathrm{ABC}} = \dfrac{Z_{\mathrm{ABC}}Y_m(k_0R_3) - \mathrm{i}Y'_m(k_0R_3)}{Z_{\mathrm{ABC}}J_m(k_0R_3) - \mathrm{i}J'_m(k_0R_3)} \end{cases} \tag{52}$$

Again, from Eq. (51), we can compute the determinant of the system P_m, which takes the same form as previously:

$$\det P_m = -\left[\varphi_m\left(\alpha_m\beta'_m - \alpha'_m\beta_m\right) + \left(\beta_m - \beta'_m\right)\right] + \varphi_{\mathrm{ABC}}\left[\varphi_m\left(\alpha_m\gamma'_m - \alpha'_m\gamma_m\right) + \left(\gamma_m - \gamma'_m\right)\right] \tag{53}$$

We now introduce a new interface in $r = R + h$, where $0 < h < d$, which splits the domain. The same transmission conditions are applied to this interface. The global system which governs the problem is (equivalently to Eq. (33)):

$$K_m = \begin{bmatrix} \varphi_m & 1 & 0 & 0 & 0 & 0 \\ \psi_{1,m} & 1 & -\psi_{1,m} & -1 & 0 & 0 \\ \psi_{2,m} & 1 & -\psi_{2,m} & -1 & 0 & 0 \\ 0 & 0 & 1 & \alpha_m & -\beta_m & -\gamma_m \\ 0 & 0 & 1 & \alpha'_m & -\beta'_m & -\gamma'_m \\ 0 & 0 & 0 & 0 & \varphi_{\mathrm{ABC}} & 1 \end{bmatrix}, \qquad f_m = \begin{bmatrix} 0 \\ 0 \\ 0 \\ 0 \\ 0 \\ i^{\mathrm{m}} \end{bmatrix} \tag{54}$$

where, this time, the parameters $\psi_{1,m}$ and $\psi_{2,m}$ are:

$$\psi_{1,m} = \frac{\sqrt{\frac{\mu}{\varepsilon}}Y'_m(kR_1) + \mathrm{i}\widehat{t_m}Y_m(kR_1)}{\sqrt{\frac{\mu}{\varepsilon}}J'_m(kR_1) + \mathrm{i}\widehat{t_m}J_m(kR_1)} \tag{55}$$

$$\psi_{2,m} = \frac{-\sqrt{\frac{\mu}{\varepsilon}}Y'_m(kR_1) + \mathrm{i}\widehat{\overline{t_m}}Y_m(kR_1)}{-\sqrt{\frac{\mu}{\varepsilon}}J'_m(kR_1) + \mathrm{i}\widehat{\overline{t_m}}J_m(kR_1)} \tag{56}$$

Let Γ_m be:

$$\Gamma_m = \frac{\varphi_{\mathrm{ABC}}(\gamma_m - \gamma'_m) - (\beta_m - \beta'_m)}{\varphi_{\mathrm{ABC}}(\gamma_m\alpha'_m - \gamma'_m\alpha_m) - (\beta_m\alpha'_m - \beta'_m\alpha_m)} \tag{57}$$

With these notations, all previous results from the infinite plane surface apply to the circle, in particular:

$$\det K_m = (\psi_{1,m} - \psi_{2,m}) \det P_m \tag{58}$$

$$Q_m = \frac{(\psi_{2,m} - \varphi_m)(\psi_{1,m} - \Gamma_m)}{(\psi_{1,m} - \varphi_m)(\psi_{2,m} - \Gamma_m)} \tag{59}$$

$$\lambda_m^{\mathrm{J}} = 1 - \frac{r_1 + r_2}{2} \pm \frac{1}{2}\sqrt{(r_1 - r_2)^2 + 4 r_1 r_2 Q_m} \tag{60}$$

$$\lambda_m^{\mathrm{GS}} = 1 - \frac{r_1 + r_2}{2} + \frac{r_1 r_2}{2} Q_m \pm \frac{1}{2}\sqrt{(r_1 - r_2)^2 - 2 r_1 r_2 (r_1 + r_2 - 2) Q_m + r_1^2 r_2^2 Q_m^2} \tag{61}$$

$$Q_m = 1 \quad \Rightarrow \quad \rho_m^{\mathrm{J}} = \rho_m^{\mathrm{GS}} = 1 \tag{62}$$

$$Q_m = 1 \quad \Leftrightarrow \quad \det P_m = 0 \quad \text{or} \quad \mathcal{R}(\widehat{t_m}) = 0 \tag{63}$$

$$\mathcal{R}(\widehat{t_m}) \not\sim m \quad \Rightarrow \quad \lim_{m\to\infty} Q_m = 1 \quad \Rightarrow \quad \lim_{m\to\infty} \rho_m = 1 \tag{64}$$

7. Application of the theoretical and spectral analysis to a finite-element context

We present in this section different numerical results of a finite-element code. This code implements the Gauss–Seidel algorithm, with relaxation on one side of the interface. The numerical modal convergence rate is to be compared to the analytical one, given by Eq. (61) with $r_1 = r$, and $r_2 = 1$:

$$\rho_{\text{modal}} = |1 - r + r Q| \tag{65}$$

where Q is given by Eq. (48) for the plane surface, and Eqs. (57), (59) for the circle.

7.1. Optimization of the coefficients, modal comparison

Besides the relaxation coefficient r, some other parameters are to be optimized. Després transmission conditions are $\partial_n u + \mathrm{i}\omega u$. We will call Després-type TC conditions with one complex parameter z written as: $\partial_n u + \mathrm{i}\omega z u$. We will call operator-type TC conditions written as $\partial_n u + \mathrm{i}\omega z(\alpha I + \beta \Lambda_0^* \Lambda_0) u$ where z is complex, α and β are real. Després-type TC have three independent optimization parameters (r, $\mathcal{R}(z)$, and $\mathcal{I}(z)$), while operator-type TC have four independent optimization parameters (r, $\mathcal{R}(z\alpha)$, $\mathcal{I}(z\alpha)$, and β/α). Operator-type TC may have a fifth parameter δ: the size of the truncation function. The objective function to minimize is the maximal convergence rate over all modes.

For Després-type TC, we know that $\rho_\infty = \lim \rho = 1$ and thus we cannot minimize over all modes. We have to restrict the minimization on a range of modes $[0; s_{\max}]$ or $[0; m_{\max}]$.

For operator-type TC, we can show that, from a certain mode s_0, the convergence rate becomes monotonous and thus minimizing $\max[\max_{s\in[0,s_0]} \rho_s; \rho_\infty]$ is equivalent to minimizing $\max_{s\in[0,\infty]} \rho_s$: it is possible to minimize the maximal rate over all modes for operator-type TC.

Fig. 2 presents the convergence rate as a function of the mode of the exciting wave (it is the modal convergence rate). The effective convergence rate of a finite element process is the maximum of these functions. The aim of the optimization is to reduce this maximum. As seen before, the infinite convergence rate for Després-type transmission conditions (optimized or not) is equal to one: see Figs. 2(a) and 2(c). On the contrary, under operator-type transmission conditions (Fig. 2(d)), we can adjust the parameters in order to equalize the different maximums of the convergence rate (basically, on simple cases, we balance the lower modes, the higher modes and the grazing modes).

7.2. Behavior of the transmission conditions against mesh refinement

The interest of non-local operator as transmission operator appears even more clearly when refining a mesh. Indeed, the finer the mesh is, the more high modes it will represent and the worst it will get for local transmission conditions. On the other hand, with non-local operators, we insure that each well-represented mode will have a convergence rate lower than a constant independent of the refinement. Fig. 3 shows such a phenomenon: it represents the evolution of the error of the solution for different mesh refinement (for 30 points per wavelength to 120 points per wavelength).

7.3. Influence of the truncation

We finally study the influence of the size of the truncation on the convergence rate. This is done numerically thanks to the analytical formulae obtained in the previous sections. The truncation function introduced previously is used to sparsify the matrix after discretization. Indeed, a non-local operator such as integral kernels required here leads after discretization to a full matrix describing the interaction on the interface. A local operator (such as derivatives) usually corresponds to three-points or five-points stencils. In our case, the truncation uses a specific length δ and then the number of points depends on the refinement. In 2D problems, the matrix will have $(2\lceil \frac{\delta}{h} \rceil + 1) * \lceil \frac{L}{h} \rceil$ non-zero elements, where δ is the length of the truncation, L that of the (1D) interface and h is the step size. The ratio $\frac{\delta}{L}$ gives the sparsity of the matrix. In Fig. 4,

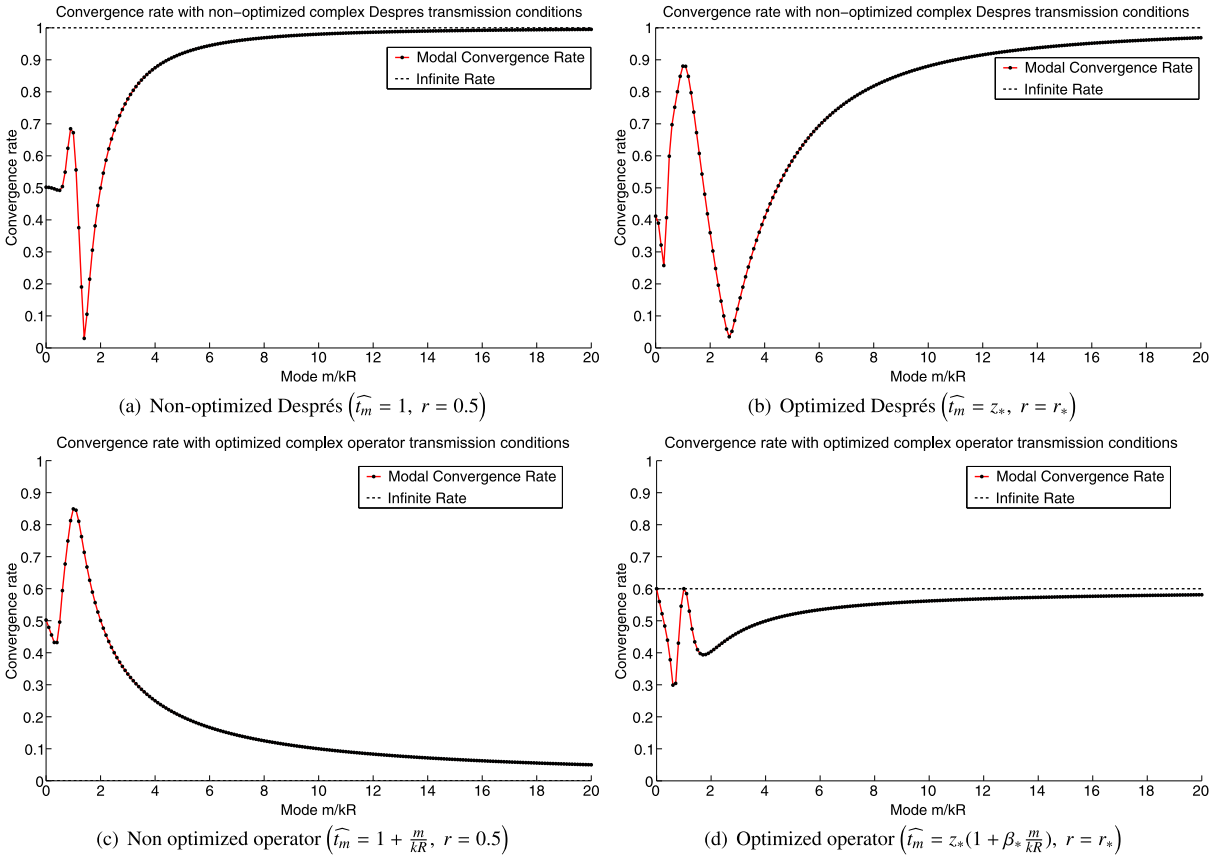

(a) Non-optimized Després $\left(\widehat{\imath_m} = 1,\ r = 0.5\right)$

(b) Optimized Després $\left(\widehat{\imath_m} = z_*,\ r = r_*\right)$

(c) Non optimized operator $\left(\widehat{\imath_m} = 1 + \frac{m}{kR},\ r = 0.5\right)$

(d) Optimized operator $\left(\widehat{\imath_m} = z_*(1 + \beta_* \frac{m}{kR}),\ r = r_*\right)$

Fig. 2. (Color online.) Convergence rate on a circle problem versus the mode $\frac{m}{kR}$. On the left (2(a)–2(c)), the transmission conditions are not optimized, while on the right (2(b)–2(d)) the conditions are optimized over $\frac{m}{kR} \in [0, 10]$. The optimization objective is to lower the maximum of the functions.

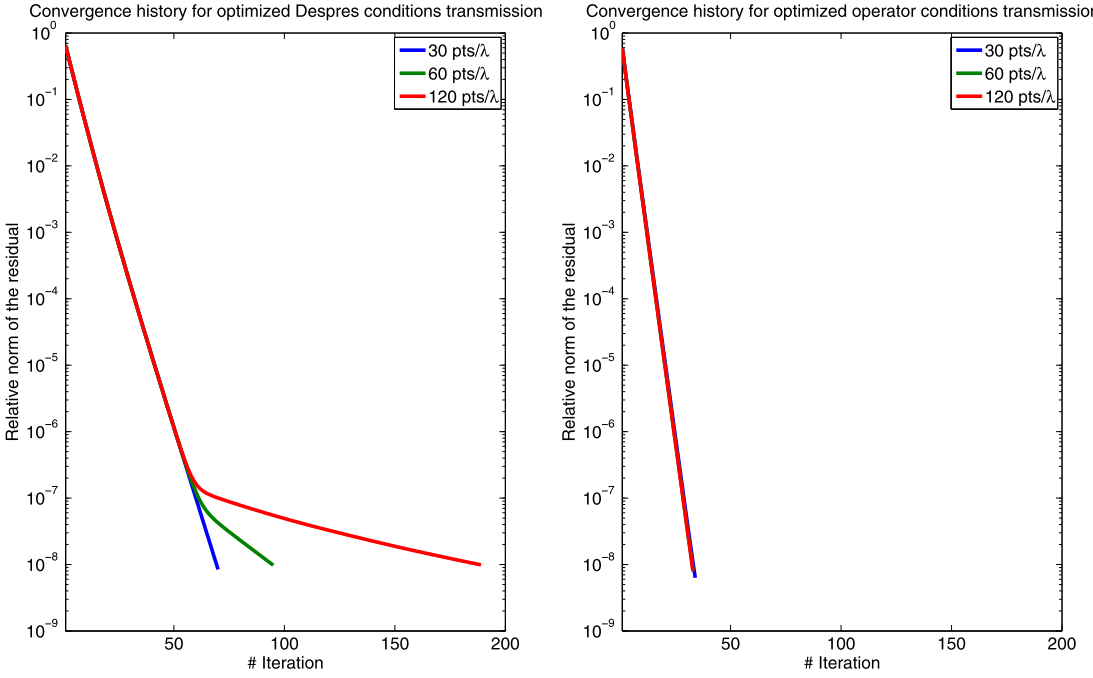

Fig. 3. (Color online.) Convergence rate for several refinement for optimized Després transmission conditions (left) and optimized operator transmission conditions. For Després TC, the convergence depends strongly on the refinement.

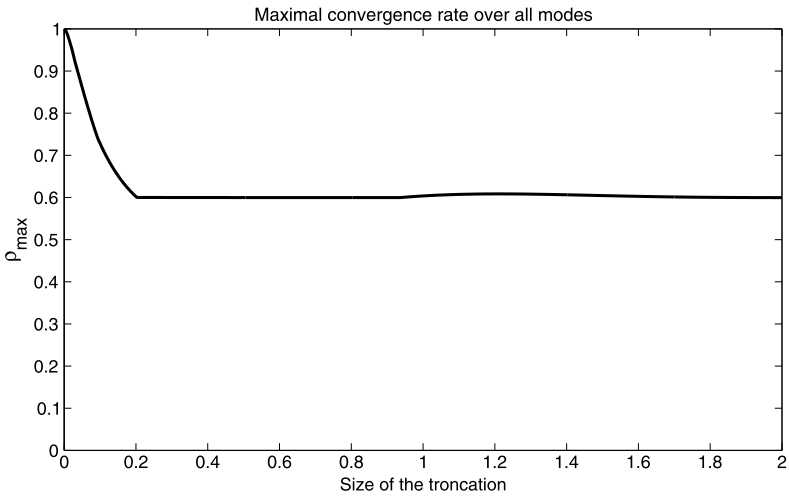

Fig. 4. Influence on the convergence rate of the length of the truncation.

we have represented the maximal convergence rate over all modes $\max_{s\in[0,\infty]} \rho_s$ (i.e. the effective convergence rate of a finite-element algorithm) as a function of the size δ of the truncation. The computation is made for the problem with circular surface. The surface of the interface is located at $r = 1.5$ and thus the length of the interface is around 10. An optimum (in the sense as small truncation as possible without degrading the convergence rate) can easily be found (around 0.2 in our case, leading to a matrix density of 2%).

8. Conclusion

In this article, we have presented new transmission conditions for domain decomposition methods. The very particular order of the transmission operator involved leads to a proven geometric convergence of a Jacobi or Gauss–Seidel algorithm. Because of their integral nature, these conditions give after discretization full matrices, but a truncation process has been introduced to address this issue without degrading the convergence. Our first theoretical and numerical results are quite promising and the interest of this method becomes more obvious when high refinement is required (high precision on the solution or small geometrical details).

Further numerical investigation, especially 3D and/or realistic cases have to be pursued, as well as the question of intersecting interfaces.

References

[1] B. Després, Domain decomposition method and the Helmholtz problem (Part II), in: Second International Conference on Mathematical and Numerical Aspects of Wave Propagation Phenomena, SIAM, 1993, pp. 197–206.
[2] M. Gander, F. Magoulès, F. Nataf, Optimized Schwarz methods without overlap for the Helmholtz equation, SIAM J. Sci. Comput. 24 (1) (2002) 38–60.
[3] Z. Peng, V. Rawat, J.-F. Lee, One way domain decomposition method with second order transmission condition for solving electromagnetic wave problems, J. Comput. Phys. 229 (2010) 1181–1197.
[4] B. Stupfel, D. Poget, Sufficient uniqueness conditions for the solution of the time harmonic Maxwell's equations associated with surface impedance boundary conditions, J. Comput. Phys. 230 (2011) 4571–4587.
[5] F. Collino, S. Ghanemi, P. Joly, Domain decomposition method for the harmonic wave propagation: a general presentation, Comput. Methods Appl. Mech. Eng. 184 (2000) 171–211.
[6] E. Stein, Singular Integrals and Differentiability Properties of Functions, Princeton University Press, 1970.
[7] Y. Saad, Iterative Methods for Sparse Linear Systems, Society for Industrial and Applied Mathematics, 2003.